Uncoupling of lifespan and reproductive tradeoffs by dietary methionine and one-carbon metabolism

Fangchao Wei
Department of Pharmacology and Cancer Biology, Duke University School of Medicine
Shiyu Liu
Duke University
Juan Liu
Duke University
Annamarie Allen
Department of Pharmacology and Cancer Biology, Duke University School of Medicine
Michael Reid
Department of Pharmacology and Cancer Biology, Duke University School of Medicine
https://orcid.org/0000-0001-6222-9538
Jason Locasale (dr.jason.locasale@gmail.com)
Duke University https://orcid.org/0000-0002-7766-3502

Article

Keywords: methionine restriction, tradeoff, folic acid, metabolomics, metabolic flux analysis, mitochondrial metabolism

Posted Date: June 15th, 2023

DOI: https://doi.org/10.21203/rs.3.rs-3031504/v1

Abstract

Aging has been proposed to be a consequence of reproductive ability and longevity thus occurs as a tradeoff with organismal reproduction[1, 2]. Lifespan extending interventions generally at the expense of fertility[3]. How this principle extends to nutrition and metabolism is not understood. We considered dietary methionine restriction (MR) that is linked to one carbon metabolism as well as to Mediterranean or plant-based diets[4 ,5] and known to influence cancer[6], metabolic health[7], and longevity[3, 8]. Using a chemically defined diet (CDD) we developed for *Drosophila melanogaster*, we found that MR-mediated lifespan extension indeed occurs at the expense of reproduction. A survey of the nutritional landscape in the background of MR revealed that folic acid, a vitamin linked to one carbon metabolism, surprisingly was the lone nutrient that restored reproductive defects without compromising lifespan extension. In vivo isotope tracing, metabolomics and flux analysis identified the Tricarboxylic (TCA) cycle and redox coupling as the primary determinants of MR benefits. Interestingly, the fecundity defect occurred through altered sperm function and its restoration by folic acid supplementation also restored sperm mitochondrial metabolism. Together these findings suggest that dietary interventions connected to specific changes in metabolism can separate adverse effects that may occur by enhancing longevity.

Introduction

Why organisms lose fitness over time and thus age is a longstanding issue. It has been proposed that aging is a necessary consequence of somatic maintenance including the need for reproductive capacity[1, 2]. Thus, commonly considered means of lifespan extension such as nutrition restriction[3] and IGF signaling reduction[9, 10] tend to result in tradeoffs to proliferation. The molecular processes that mediate this antagonism, particularly as they relate to metabolism and their potential for separability, which would be desirable if any such intervention were to be considered in practice, are largely unknown[10, 11]. One notable intervention that yields a consistent conserved lifespan extension (along with anti-cancer[6], anti-obesity[12] and anti-diabetic properties[13]) is dietary methionine restriction[3, 8]. How methionine metabolism is affected during the aging process and what tradeoffs may result are not generally known. One limitation has been technology available to study nutrition in large scale systematic ways. An attractive model is *Drosophila melanogaster* as, in addition to its established utility in aging studies[3, 8], there may exist possibilities to create synthetic diets that allow for controlled manners to survey diet and metabolism.

Methionine restriction (MR) extends lifespan at the expense of reproduction in Drosophila

To investigate nutrition and metabolism systematically, we developed a modified CDD for the fruit fly *Drosophila Melanogaster*[14–17]. To test its utility, we fed *Drosophila* for the entirety of their lifespan with the CDD, or standard cornmeal- or yeast-based diets (Extended Data Fig. 1a). Either no or modest differences in lifespan (Extended Data Fig. 1b), fertility (Extended Data Fig. 1c), eclosion time (Extended Data Fig. 1d), climbing ability (Extended Data Fig. 1e), and body weight (Extended Data Fig. 1f) were

observed, consistent with previous results[15]. A panel of diets containing differing amounts of methionine could then be constructed and their effects on health and lifespan investigated (Fig. 1a and Extended Data Fig. 2a). Lifespan was found to be dose dependent with low concentrations reducing lifespan and an optimal lifespan extension occurring at around 10% of the standard diet and concentrations up to 50% surprisingly continuing to exhibit significant effects on increased lifespan (Fig. 1b). Concomitantly, lowering the levels of methionine reduced egg production with zero methionine resulting in the fewest number of offspring (Fig. 1c and Extended Data Fig. 2b). Meanwhile 2-week windows of a 10% methionine diet at earlier ages (weeks 0, 2, 4, or 6) extended lifespan incrementally (Extended Data Figs. 3a–d, 3f-i) but not in older flies (week 8) (Extended Data Figs. 3e, 3j), and lifespan extension comes with reduced fertility (Extended Data Figs. 2c, 2g). Importantly the findings were sex independent (Figs. 1d-h, Extended Data Figs. 2d-f, 2h-j, and Extended Data Fig. 3) and lifespan extension with reduced fecundity was also observed when MR was administered at later ages to either sex (Figs. 1i-m). Thus, dietary methionine extends longevity while maintaining health span at the expense of fertility.

MR restores redox balance and enhances TCA flux that decline during aging

Methionine is a nutrient metabolized in one carbon metabolism. Its impact can occur through numerous metabolic processes[7]. Altered metabolism is a key feature of aging to but the general processes are not known[18]. Thus we sought to investigate changes to metabolism during aging and next how they are influenced by dietary methionine (Fig. 2a). Using liquid chromatography coupled with high resolution mass spectrometry, we generated metabolite profiles (Extended Data Fig. 4a) of young and old flies having eaten an MR or control CDD (Fig. 2a) and observed differences between the young and old (Extended Data Figs. 4b-d). As expected, methionine related metabolites were suppressed in MR treated young and old flies (Fig. 2b). Prominently, redox (Fig. 2c), energy (Fig. 2d), and nucleotide (Fig. 2e) related metabolites were altered as observed in other contexts MR[6, 19]. Importantly, the ratio of oxidized to reduced glutathione and NAD^+/NADH cytosolic redox ratio (Fig. 2c), the ATP/AMP ratio a measure of energy status (Fig. 2d), and levels of di- and tri phosphate nucleotides (Fig. 2e) were each restored to levels in young animals by MR in aging animals. Those findings are consistent with studies on the beneficial effects of reducing oxidation status and promoting energy balance on lifespan extension[20–22].

To further study these metabolic effects, we modified our CDD to incorporate heavy isotopes into the diet (Fig. 2f). We first fed flies with U-^{13}C-Methionine to investigate methionine cycle flux and developed a computational scheme to quantify methionine flux (Fig. 2g, methods). This revealed increased methionine cycling activity during MR in young and old flies indicating compensatory methyl donor availability during MR. With U-^{13}C-Sucrose and a computational, artificial intelligence-based method of determining fluxes from isotope tracing (Fig. 2h, methods), we assessed metabolic fluxes in central carbon metabolism. We found that consistent with changes to redox, energy and nucleotide metabolism,

MR enhanced TCA cycle activity in young and old (Fig. 2i). Altogether these findings indicate that enhanced TCA cycle activity is the major effect of MR.

Folic acid (FA) supplementation uncouples the lifespan-fertility tradeoff induced by MR

To investigate the generality of this tradeoff induced by MR, we surveyed the nutritional landscape in the background of a lifespan extending but fertility decreasing dose of MR (Fig. 3a). We supplemented the methionine restricted diet with an array of nutrients in broad categories such as amino acids, vitamins, and sugar, as well as nutrients specific to one carbon metabolism such as serine and folic acid (FA). In nearly all situations, increasing dietary nutrient availability suppressed lifespan extension (Fig. 3b) with the lone exception being FA supplementation which was able to maintain the lifespan effect. The addition of FA alone led to no changes in the lifespan and the effects of FA on maintaining lifespan extension in the background of MR could be achieved under high doses (up to 200 x tested) of FA indicating that FA by itself functioned in the MR background and was not additive (Fig. 3c and Extended Data Fig. 5a). The deficiency of egg production surprisingly was completely restored (Fig. 3d) implying the MR-induced lifespan-fecundity tradeoff could be separated by FA supplementation. Five times the regular dose of FA was found to be optimal for maintaining longevity and restoring fertility (Figs. 3c, 3d). Interestingly, these effects could be obtained even when males alone were fed the diets while females were fed a control diet (Figs. 3e, 3f) and could be observed in aging flies (Figs. 3g, 3h). To exclude the involvement of gut microbiota-produced FA, we administered antibiotics into the diet[23], demonstrating that the effect is coming from dietary FA (Extended Data Figs. 5b-e). We then investigated the features of metabolism that are linked to this finding. Glycolytic flux was attenuated but TCA cycle flux enhanced (Fig. 3i), in large part due to decreasing the demand for carbon units from glycolysis together suggesting that FA supplementation during MR enhances mitochondrial function. Thus, the lifespan fecundity tradeoff apparent under MR can be uncoupled and FA is the determinant of its separability.

FA supplementation rescues MR induced sperm viability and transfer decline

Given the reproductive effects could be observed from MR administered exclusively to males, we investigated the young and old flies that were fed control, MR, MR-FA and FA diets, and sperm was assay (Fig. 4a). To test whether spermatogenesis and mature sperm count were affected, testes[24, 25], and sperm numbers in the seminal vesicle[26] were evaluated (Fig. 4b). No differences in spermatogenesis (Extended Data Fig. 6) and sperm number in the seminal vesicle (Fig. 4c) was observed. However, sperm numbers declined during aging (Fig. 4c). We next assayed sperm viability[27, 28], and found that MR reduced, and FA supplementation rescued sperm viability (Fig. 4d). This led us to investigate sperm count in the female seminal receptacle[28] (Fig. 4e). It was found that MR did indeed reduce sperm number in the receptacle and this defect was fully rescued with FA supplementation (Fig. 4f). These findings indicate that sperm

viability is the major source of reproductive defects along with the recovery induced by FA supplementation.

MR-FA maintains sperm redox balance and enhances sperm energy metabolism

Metabolically, sperm has a few specifications, and recent studies have shown[29] that sperm can rapidly respond to changes in diet. We therefore investigated the metabolism of *Drosophila* sperm in vivo by feeding flies isotopically labeled nutrients and collecting sperm (Fig. 5a). We generated metabolite profiles that are different between young and old (Extended Data Fig. 7a). Methionine related metabolites were rescued by FA (Fig. 5b) as was cytosolic redox ratio (Fig. 5c) and energy status (Fig. 5d) but not glutathione based redox (Fig. 5c) or methionine cycle flux (Fig. 5f) which we initially suspected. Defects in polyamine metabolism were rescued by FA in old flies, but not in young flies (Fig. 5e). Central carbon metabolism however was rescued by FA indicating that TCA cycle flux consistent with observations with metabolite levels was the main source of the metabolic defects (Fig. 5g and Extended Data Fig. 7b). Together these results map the metabolism of sperm in vivo and show the effects of both MR and the aspects of FA supplementation that rescued the sperm metabolism and function.

Discussion

Our finding that dietary MR extends lifespan at the expense of reduced fertility is consistent with the lifespan and fertility trade-off theory of aging. However, a survey of the dietary landscape in the background of MR found, in contrast to all other diets considered, that FA supplementation not only maintained the lifespan extended by MR but also reversed the reduced fertility. Interestingly, the reproductive effects occurred through the sperm, and by analyzing metabolism in vivo with metabolite profiling, isotope tracing, and machine learning assisted flux analysis, we found that redox balance and the restoration/maintenance of TCA cycle metabolism homeostasis, in general, were the factors influencing both sperm function and the longevity phenotype induced by MR (Fig. 5h). These findings may have several implications. They show for example how a conserved metabolic pathway that can be modified by diet influences longevity, and confirm that reproductive deficiency can, in this case by vitamin supplementation, be separated from lifespan extension through effects on the male.

Methods

Fly stocks and maintenance

Wild-type fruit fly *Drosophila melanogaster* w^{1118} strains were utilized in all experiments and sourced from the Bloomington Stock Center. The flies were maintained under standardized conditions, a temperature of 25°C and relative humidity of 60%, with a 12-hour light/12-hour dark photoperiod. Flies were collected as experimental within 8 hours post-eclosion, with 25 individuals per vial. Each vial diet was replaced with fresh provisions every 2–3 days.

Diet

The cornmeal diet was obtained from Genesee Scientific (# 66–112), while the yeast-based diet was modified from previously published recipes[30, 31]. Chemically Defined Diet (CDD) was prepared and modified based on previous research[14–17]. Variations of the CDD, including methionine-restricted diets, nutrient-enriched diets, a sulfa quinoxaline-added diet, and isotope tracing diets (U-^{13}C5-Methionine and U-^{13}C6-Sucrose (Fructose)) were also developed. Diets can be stored at 4°C for several weeks (after which they will shrink due to loss of water and pull away from the side of the vial).

Egg counting and egg development time

Mated female flies were transferred to fresh diet vials every day to allow for observation of egg production and egg development time. Egg counting from the 3rd day after mating lasts for 30 days.

Climbing activity and body weight

Fly climbing activities were assessed referring to a previously described[32]. Shortly, 10 single-sex flies, were transferred to an empty standard 23 × 95 mm plastic vial and then gently tapped to the bottom 3 times. The number of flies that reached the top vial within 20 seconds was then scored as climbing. Consecutive trials were separated by 1 minute of rest, and each experiment was performed on a minimum of 3 vials of 10 flies per condition repeated 3 times. Test every 5–10 days and follow up for 2 months.

For body weight, 50 flies were collected, weighed every 10 days, and followed up for 2 months. Each experiment was performed on at least 150 flies (3 vials of 50 flies per condition) and repeated 3 times.

Lifespan assessment

Flies were collected within 8 hours after eclosion and sorted under CO_2 anesthesia. The individuals were then randomly assigned to various feeding regimes, with 25 single-sex flies placed in each vial. Throughout the experiment, the flies were transferred to a fresh vial containing the corresponding diet every 2–3 days. Mortality was monitored daily by checking for dead flies in the vials and recording the number of deaths.

Folic acid concentration assay

Diets or 100 flies were prepared and quantified according to the Folic Acid Concentration Assay Kit (Novus Biologicals NBP2-82433).

Tissue preparation

Separation of the male reproductive system, which consists of the testes, seminal vesicles, accessory glands, and ejaculatory duct. Separation of the female reproductive system, which consists of the bursa,

spermatheca, seminal receptacle, and ovaries. Tissues were observed or stored at -80°C for future experiments.

Sperm was isolated as in previous studies[27–29]. The seminal vesicle and ejaculatory duct (90 minutes after mating) were separated from the male reproductive system and torn using a dissecting needle. The tissue was placed into a centrifuge tube containing 300 µl of ddH_2O and mixed for 10 minutes at room temperature (RT), seminal vesicles and ejaculatory duct were discarded, and the sperm was centrifuged at 3000 rpm for 5 minutes at RT. Save the pelleted sperm for mass spectrometry or store it at -80°C for future use.

Testes staining

The male reproductive system was dissected, and removed the seminal vesicles, glands, and ejaculatory duct. *W^{1118}* male testes were harvested and dissected in PBS and fixed in 5% formaldehyde for 20 minutes, followed by washing in PBS + 0.1% Triton X-100 for 15 minutes. The samples were stained as described[26], with rhodamine-phalloidin (0.1 µM, Sigma-Aldrich, P1951) and DAPI (10 µM, Invitrogen D1306) for 20 minutes. The images were captured using a Zeiss LSM510 confocal motorized inverted microscope with an XM-10 monochrome camera.

Sperm number and sperm viability

Put the isolated seminal vesicles or seminal receptacle in 5–10 µl of PBS. The tissue was punctured using a dissecting needle and allowed to rest for 10 minutes to release the sperm. Stain with DAPI or SYBR[28, 29]. DAPI staining resulted in the blue staining of the sperm heads, while SYBR staining produced green fluorescence in live sperm and red fluorescence in membrane-compromised sperm when used in conjunction with propidium iodide. The SYBR staining procedure was carried out as follows: Sperm samples were diluted in a live-cell imaging solution that contained 10% BSA. A stock solution of SYBR 14 dye was created by adding 900 µl of DMSO. Then, 1 µl of the SYBR 14 stock solution and 5 µl of propidium iodide solution were mixed with the diluted sperm sample. The mixture was incubated at 37°C for 5–10 minutes, following which the sample was observed using a confocal microscope.

Metabolite extraction

10 flies or 30 (young)/90 (old) flies' sperm were collected under light CO_2 anesthesia and rapidly frozen in liquid nitrogen. The frozen flies were then ground using a CryoMill. Metabolite extraction was performed as described in the previous study[33]. The supernatant was transferred to a new Eppendorf tube and dried in a vacuum concentrator at RT. The dry pellets were reconstituted into 30 µl sample solvent (15 µl water and then 15 µl methanol/acetonitrile (1:1 v/v)) and 3 µl was further analyzed by liquid chromatography coupled to high resolution mass spectrometry. Mobile phase A is water with 5 mM ammonium acetate, pH 6.9, and mobile phase B is 100% acetonitrile.

An Ultimate 3000 UHPLC (Dionex) was coupled to Q Exactive-Mass Spectrometer (QE-MS, Thermo Scientific) for metabolite separation and detection. For metabolite analysis, used a HILIC method, with an

Xbridge amide column (100 × 2.1 mm internal diameter, 3.5 µm; Waters), for compound separation at RT. The mobile phase and gradient information have previously been described[33]. The gradient is linear as follows: 0 minute, 85% B; 1.5 minutes, 85% B; 5.5 minutes, 35% B; 10 minutes, 35% B; 10.5 minutes, 35% B; 10.6 minutes, 10% B; 12.5 minutes, 10% B; 13.5 minutes, 85% B; and 20 minutes, 85% B. The flow rate is 0.15 ml/minute from 0 to 5.5 minutes, 0.17 ml/minute from 6.9 to 10.5 minutes, 0.3 ml/minute from 10.6 to 17.9 minutes, and 0.15 ml/minute from 18 to 20 minutes. The QE-MS is equipped with a heated electrospray ionization probe, and the relevant parameters are listed: evaporation temperature, 120°C; sheath gas, 30; auxiliary gas, 10; sweep gas, 3; spray voltage, 3.6 kV for positive mode and 2.5 kV for negative mode. The capillary temperature was set at 320°C, and S-lens was 55. A full scan ranges from 70 to 900 (m/z) was used. The resolution was set at 70,000. The maximum injection time was 200 ms. Automated gain control was targeted at 3 x 10^6 ions.

Polyamine extraction

Metabolite extraction was performed as described in previous study[34]. The supernatant was transferred to a new Eppendorf tube and dried in vacuum concentrator at RT. The dry pellets were reconstituted into 30 µl sample solvent (water: initial gradient, 1:4, v/v) and 3 µl was further analyzed by LC-MS. Initial gradient is 99% A (2 mM ammonium acetate in 10% (v/v) acetonitrile) plus 1% B (0.4% (v/v) acetic acid in 10% (v/v) acetonitrile).

Ultimate 3000 UHPLC is coupled to QE-MS for polyamine profiling. A pH gradient-liquid chromatography method employing a Scherzo SM-C18 column (50 x 2.0 mm i.d., 3 µm; Imtakt, Japan) at 30 ^oC is used for polyamine separation[34]. The linear gradient used is as follows: 0 min, 1% B; 1 minute, 5% B, 3 minutes, 5% B; 5 minutes, 100% B, 10 minutes, 100% B. The flow rate is 0.2 ml/minute. Then the system is washed with 100% B for 10 minutes at flow rate 0.2 ml/minute to wash polyamine carryover. Repeat this washing step 4 times, then equilibrate column for 10 minutes with 1% B before analyzing next polyamine sample. The equilibrium step right before sample analysis is crucial as initial condition significantly impacts polyamine separation. The QE-MS is equipped with a HESI probe with related parameters set as below: heater temperature, 120°C; sheath gas, 30; auxiliary gas, 10; sweep gas, 3; spray voltage, 3.0 kV at positive mode; capillary temperature, 320°C; S-lens, 55; A scan range (m/z) of 70 to 240 was used in positive mode from 0.5 to 9 minutes; resolution: 70000; automated gain control (AGC), 3 × 10^6 ions. Customized mass calibration was performed before data acquisition.

Metabolomics data processing and metabolic flux analysis (MFA)

Analytical LC-MS peak extraction and integration were performed using commercially available software Sieve 2.2 (Thermo Scientific). The integrated peak intensities were used for further data analysis. Natural abundance was corrected as previously described[35] for tracing studies.

We constructed methionine and one-carbon metabolic flux analysis (MFA). By setting flux values, as weights to a group of flux values, predict the mass isotopomer distribution (MID) of target metabolites by

an average of the MID of the precursors. Mode as:

$$\widetilde{M}_i = \frac{\sum_{\forall j} v_{ji} M_{ji}}{\sum_{\forall j} v_{ji}}$$

$\widetilde{\boldsymbol{M}}_i$: predicted MID vector of metabolite i; $\boldsymbol{M}_{ji}$: MID of metabolite i produced from a substrate j, and v_{ji} from j to i. Noised MID data is generated from normal simulated MID data. 20% uniformly random noise is added to each element of MID, and then the perturbed MID is normalized again to be the noisy data set. The difference between the predicted and experimental MIDs was evaluated by Kullback–Leibler divergence:

$$L_i = D_{\mathrm{KL}}\left(\widetilde{M}_i \parallel M_i\right) = \sum_j \left(M_{i,j} + \epsilon_{\log}\right) \log \frac{\widetilde{M}_{i,j} + \epsilon_{\log}}{M_{i,j} + \epsilon_{\log}}$$

$M_{i,j}$ and $\widetilde{M}_{i,j}$ are element j in vector M_i and $\widetilde{M}_i$, respectively. $\epsilon_{\log}$ is a small number added to maintain numerical stability. Sum of L_i for all target metabolites was regarded as the loss function L_{total} to minimize. The optimization problem was defined as:

$$\min_v L_{\mathrm{total}}(v), \mathrm{s.t.}\ A \bullet v^T = b, 0 \le v_{\min} \le v \le v_{\max}$$

$A \bullet v^T = b$: represents flux balance requirement and other equality constraints. $v_{\min}$ and $v_{\max}$ are lower and upper bounds for composite vector v. The optimization method refers to previous publication[36, 37].

To reduce random errors in batch preparation and measurement, MIDs in all biological repeats are averaged to be the target MID for MFA. Network diagrams with flux values are plotted with the Python package Matplotlib, the directions of a flux arrow are set by directions of net flux, and the transparency of flux arrows is set based on its value.

Statistical analysis and bioinformatics

Analysis of metabolites was carried out with software Metaboanalyst (http://www.metaboanalyst.ca/MetaboAnalyst/) and software GENE-E (https://software.broadinstitute.org/GENE-E/) using the Kyoto Encyclopedia of Genes and Genomes (KEGG) pathway database (http://www.genome.jp/kegg/). All data are represented as Mean ± s.e.m. as indicated. *P* values were calculated by a two-tailed Student's t test unless otherwise noted. All experiments were performed in at least three biological replicates and repeated in two to three independent experiments. Prism 7 (GraphPad) was used to perform statistical analysis.

Declarations

Acknowledgments

Support from the National Institutes of Health grant (R01CA193256) (J.W.L.) is gratefully acknowledged. We gratefully acknowledge members of the Locasale lab for helpful discussions and apologize to those whose work we did not cite due to space constraints.

Author Contributions

J.W.L. and F.C.W. designed the study. J.W.L. and F.C.W. wrote and edited the paper. F.C.W. performed the experiments and the data analysis. S.Y.L. designed and optimized the calculation method of metabolic flux. J.L. assisted in metabolomics data analysis. A.E.A., and M.A.R. optimized the chemically defined diet.

Competing interests

J.W.L. and F.C.W. have one pending patent application. All other authors declare no competing interests.

Data and Material Availability

All data needed to evaluate the conclusions are present in the paper and the Extended Data Materials. Metabolomics data are available on GITHUB via https://github.com/LocasaleLab/MR-FA 2023.

References

1. Westendorp RG, Kirkwood TB. Human longevity at the cost of reproductive success. *Nature*. 396, 743-746 (1998).
2. Kirkwood TB. Understanding the odd science of aging. *Cell*. 120, 437-447 (2005).
3. Grandison RC, Piper MD, Partridge L. Amino-acid imbalance explains extension of lifespan by dietary restriction in *Drosophila*. *Nature*. 462, 1061-1604 (2009).
4. Tosti V, Bertozzi B, Fontana L. Health benefits of the Mediterranean diet: Metabolic and Molecular Mechanisms. *J. Gerontol A Biol Sci Med Sci.* 73, 318–326 (2018).
5. Dai Z, Zheng W, Locasale JW. Amino acid variability, tradeoffs and optimality in human diet. *Nat Commun.* 13, 6683 (2022).
6. Gao X, et al. Dietary methionine influences therapy in mouse cancer models and alters human metabolism. *Nature*. 572, 397-401 (2019).
7. Sanderson SM, et al. Methionine metabolism in health and cancer: a nexus of diet and precision medicine. *Nat Rev Cancer*. 19, 625-637 (2019).
8. Lee BC, et al. Methionine restriction extends lifespan of *Drosophila melanogaster* under conditions of low amino-acid status. *Nat Commun*. 5, 3592 (2014).

9. Dillin A, Crawford DK, Kenyon C. Timing requirements for insulin/IGF-1 signaling in *C. elegans*. *Science*. 298 (5594), 830-834 (2002).
10. Khan J, et al. Mechanisms of ageing: growth hormone, dietary restriction, and metformin. *The lancet. Diabetes & endocrinology*, 11, 261–281 (2023).
11. Hsin H, Kenyon C. Signals from the reproductive system regulate the lifespan of *C. elegans*. *Nature*. 399, 362–366 (1999).
12. Ables GP, et al. Methionine-restricted C57BL/6J mice are resistant to diet-induced obesity and insulin resistance but have low bone density. *PLoS One*. 7(12): e51357 (2012).
13. Castaño-Martinez T, et al. Methionine restriction prevents onset of type 2 diabetes in NZO mice. *FASEB J*. 33(6): 7092-7102 (2019).
14. Troen AM, et al. Lifespan modification by glucose and methionine in *Drosophila melanogaster* fed a chemically defined diet. *Age (Dordr)*. 29, 29-39 (2007).
15. Piper MD, et al. A holidic medium for *Drosophila melanogaster*. *Nat Methods*. 11, 100-105 (2014).
16. Gu X, et al. Sestrin mediates detection of and adaptation to low-leucine diets in *Drosophila*. *Nature*. 608, 209-216 (2022).
17. Allen AE, et al. Nucleotide metabolism is linked to cysteine availability during ferroptosis. *J Biol Chem*. 299, 103039 (2023).
18. Reinke BA, et al. Diverse aging rates in ectothermic tetrapods provide insights for the evolution of aging and longevity. *Science*. 376, 1459-1466 (2022).
19. Mentch SJ, et al. Histone methylation dynamics and gene regulation occur through the sensing of one-carbon metabolism. *Cell Metab*. 22, 861-73 (2015).
20. Zhang H, et al. NAD repletion improves mitochondrial and stem cell function and enhances life span in mice. *Science*. 352, 1436-1443 (2016).
21. Yaku K, Okabe K, Nakagawa T. NAD metabolism: Implications in aging and longevity. *Ageing Res Rev*. 47, 1-17 (2018).
22. Xu M, et al. Dietary nucleotides extend the life span in Sprague-Dawley rats. *J Nutr Health Aging*. 17, 223-229 (2013).
23. Blatch SA, Meyer KW, Harrison JF. Effects of dietary folic acid level and symbiotic folate production on fitness and development in the fruit fly *Drosophila melanogaster*. *Fly (Austin)*. 4, 312-319 (2010).
24. Sitaram P, Hainline SG, Lee LA. Cytological analysis of spermatogenesis: live and fixed preparations of *Drosophila* testes. *J Vis Exp*. 83, e51058 (2014).
25. David GB, Miller E, Steinhauer J. *Drosophila* spermatid individualization is sensitive to temperature and fatty acid metabolism. *Spermatogenesis*. 5, e1006089 (2015).
26. McCullough EL, et al. The life history of *Drosophila* sperm involves molecular continuity between male and female reproductive tracts. *Proc Natl Acad Sci U S A*. 119, e2119899119 (2022).
27. Holman L. *Drosophila melanogaster* seminal fluid can protect the sperm of other males. *Functional Ecology.* 23, 180-186 (2009).

28. Sepil I, et al. Male reproductive aging arises via multifaceted mating-dependent sperm and seminal proteome declines, but is postponable in *Drosophila*. *Proc Natl Acad Sci U S A.* 117, 17094-17103 (2020).
29. Nätt D, et al. Human sperm displays rapid responses to diet. *PLoS Biol*. 17, e3000559 (2019).
30. Carvajal V, Faisal AA, Ribeiro C. Internal states drive nutrient homeostasis by modulating exploration-exploitation trade-off. *eLife*. 5, e19920 (2016).
31. Steck K, et al. Internal amino acid state modulates yeast taste neurons to support protein homeostasis in *Drosophila*. *eLife*. 7, e31625 (2018).
32. Ulgherait M, et al. Circadian autophagy drives iTRF-mediated longevity. *Nature*. 598, 353–358 (2021).
33. Liu X, Ser Z, Locasale JW. Development and quantitative evaluation of a high-resolution metabolomics technology. *Anal Chem.* 86, 2175-2184 (2014).
34. Cho H, et al. pH gradient-liquid chromatography tandem mass spectrometric assay for determination of underivatized polyamines in cancer cells. *J Chromatogr B Analyt Technol Biomed Life Sci.*1085, 21-29 (2018).
35. Liu X, et al. Metformin targets central carbon metabolism and reveals mitochondrial requirements in human cancers. *Cell Metab*. 24, 728-739 (2016).
36. Antoniewicz M, et al. Elementary metabolite units (EMU): a novel framework for modeling isotopic distributions. *Metabolic engineering*. 9, 68-86 (2007).
37. Kraft, D. A software package for sequential quadratic programming. Forschungsbericht- Deutsche Forschungs- und Versuchsanstalt fur Luft- und Raumfahrt (1988).

Figures

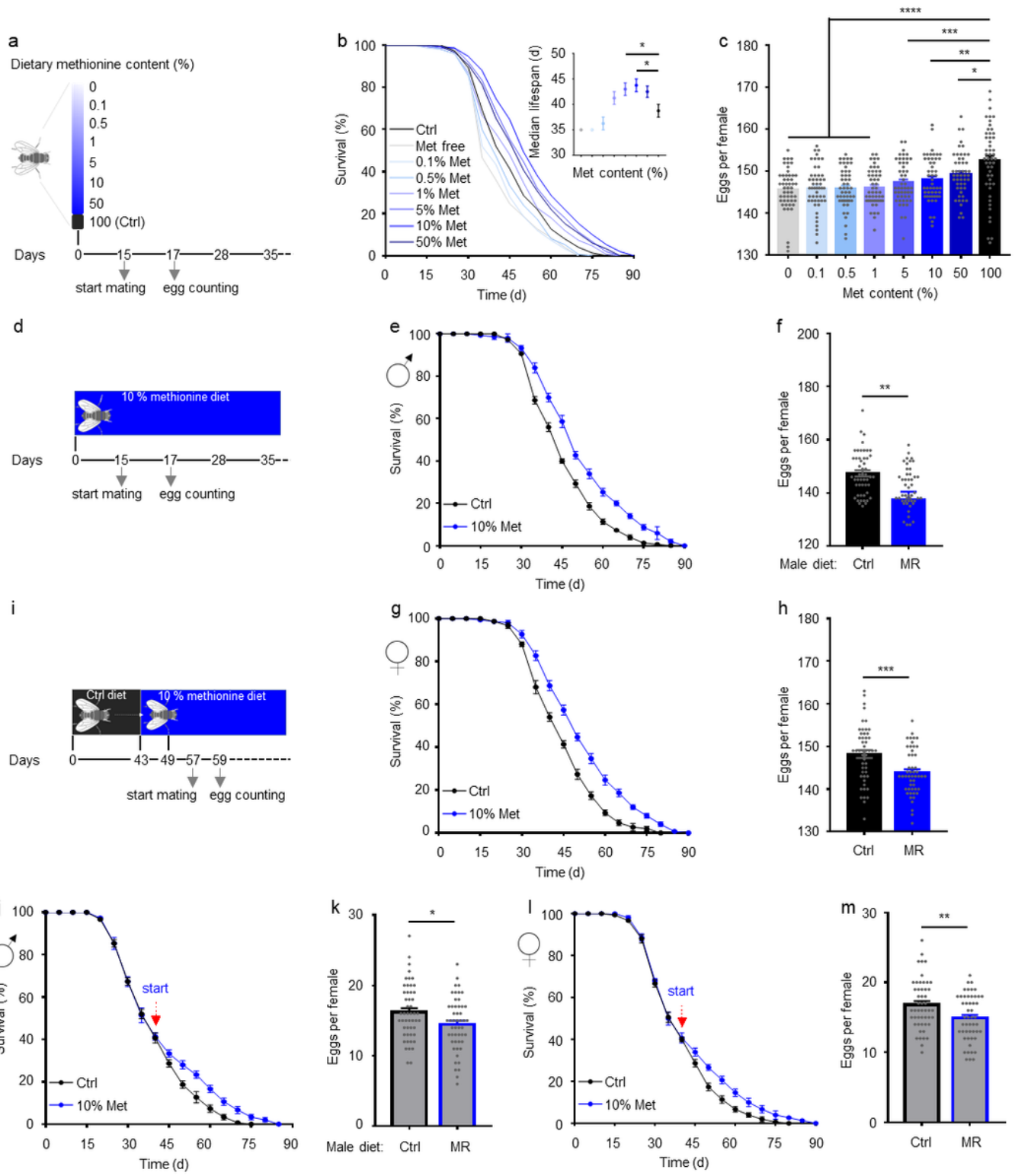

Figure 1

Methionine restriction (MR) extends lifespan at the expense of reproduction in *Drosophila*. (a) Schematic of methionine restriction (MR) diets. (b) Lifespan on MR diet. (c) Egg production in females as a function of methionine concentration. (d-m), Schematic of 10% methionine dietary exposure in young (d) and old (i) *Drosophila*. 10% methionine diet extends lifespan of male (e, j) and female (g, l), and reduces

reproduction of male (f, k) and female (h, m). n=50 flies per group. Mean ± s.e.m. *P < 0.05, **P < 0.01, ***P< 0.001 and ****P < 0.0001. P values were obtained by unpaired, two-tailed t-test.

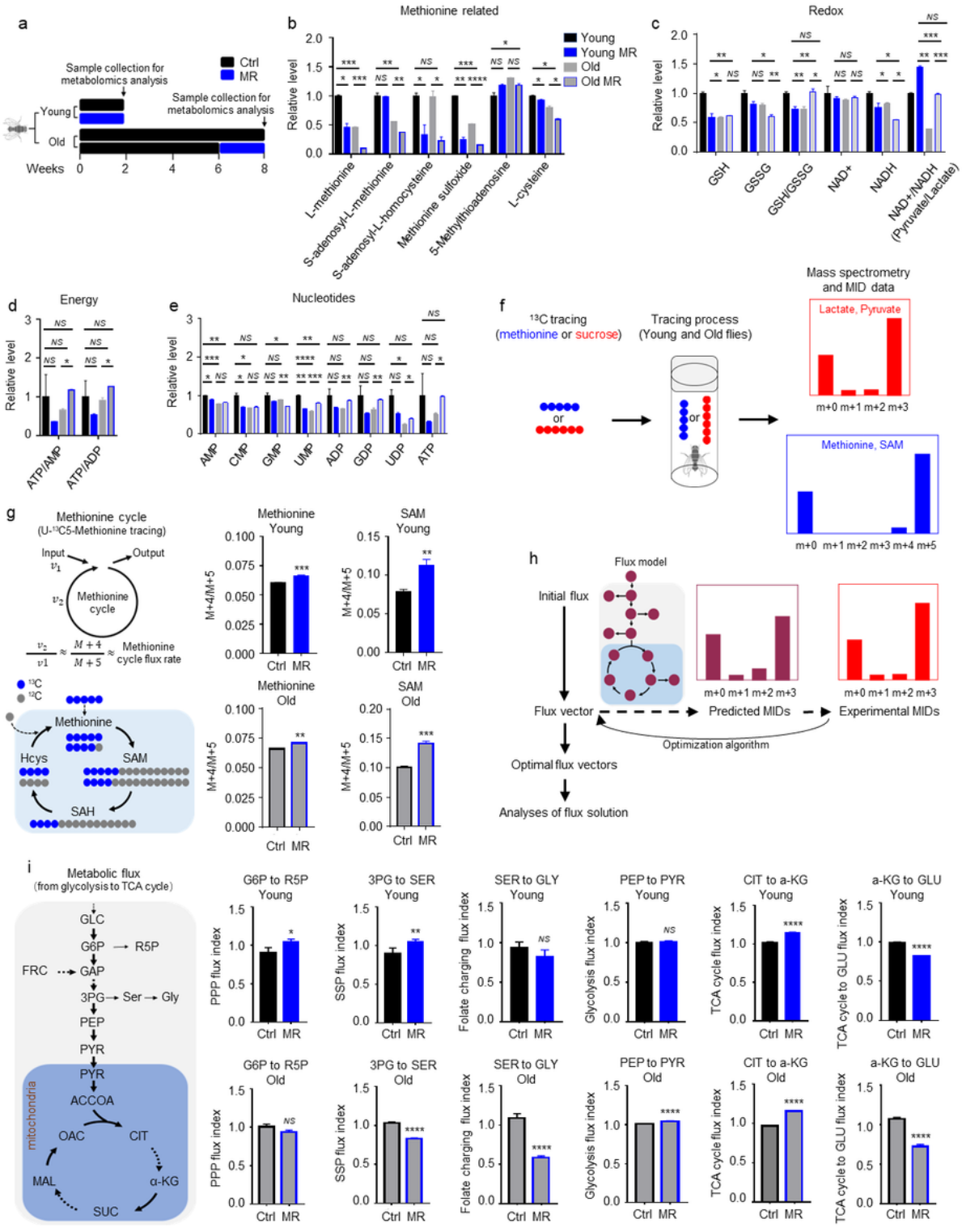

Figure 2

MR restores redox balance and enhances TCA flux. (a) Experimental design. (b-e), Metabolites related to methionine (b), redox balance (c), energy status (d) and nucleotides (e). (f) ^{13}C tracing experimental

design. (g) Methionine cycle flux analysis. (h) Central carbon metabolic flux analysis experimental design. (i) Central carbon metabolic flux analysis. n=30 flies per group. Mean ± s.e.m. *NS* = $P > 0.05$, *$P < 0.05$, **$P < 0.01$, ***$P < 0.001$ and ****$P < 0.0001$. *P* values were obtained by unpaired, two-tailed *t*-test.

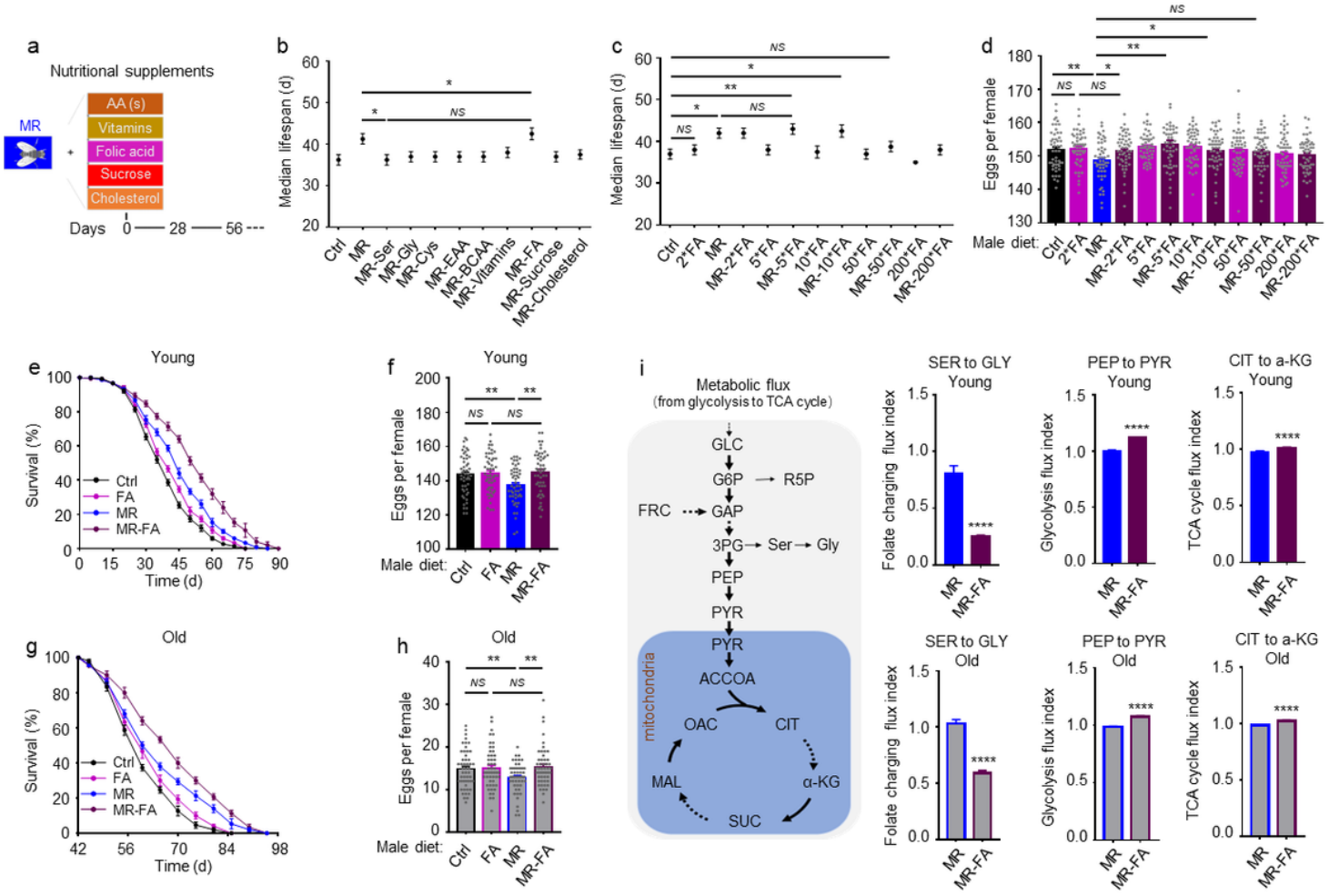

Figure 3

Folic acid (FA) supplementation uncouples the lifespan-fecundity tradeoff induced by MR. (a) Experimental design. (b) Median lifespan on different diets. (c) Median lifespan under differing doses of folic acid (FA) supplementation. (d) Egg production under differing doses of FA supplementation. (e-h) Lifespan and reproduction of young (e, f) and old (g, h) flies. (i) Central carbon metabolic flux analysis. n=30. n=50 flies per group. Mean ± s.e.m. *NS* = $P > 0.05$, *$P < 0.05$, **$P < 0.01$ and ****$P < 0.0001$. *P* values were obtained by unpaired, two-tailed *t*-test.

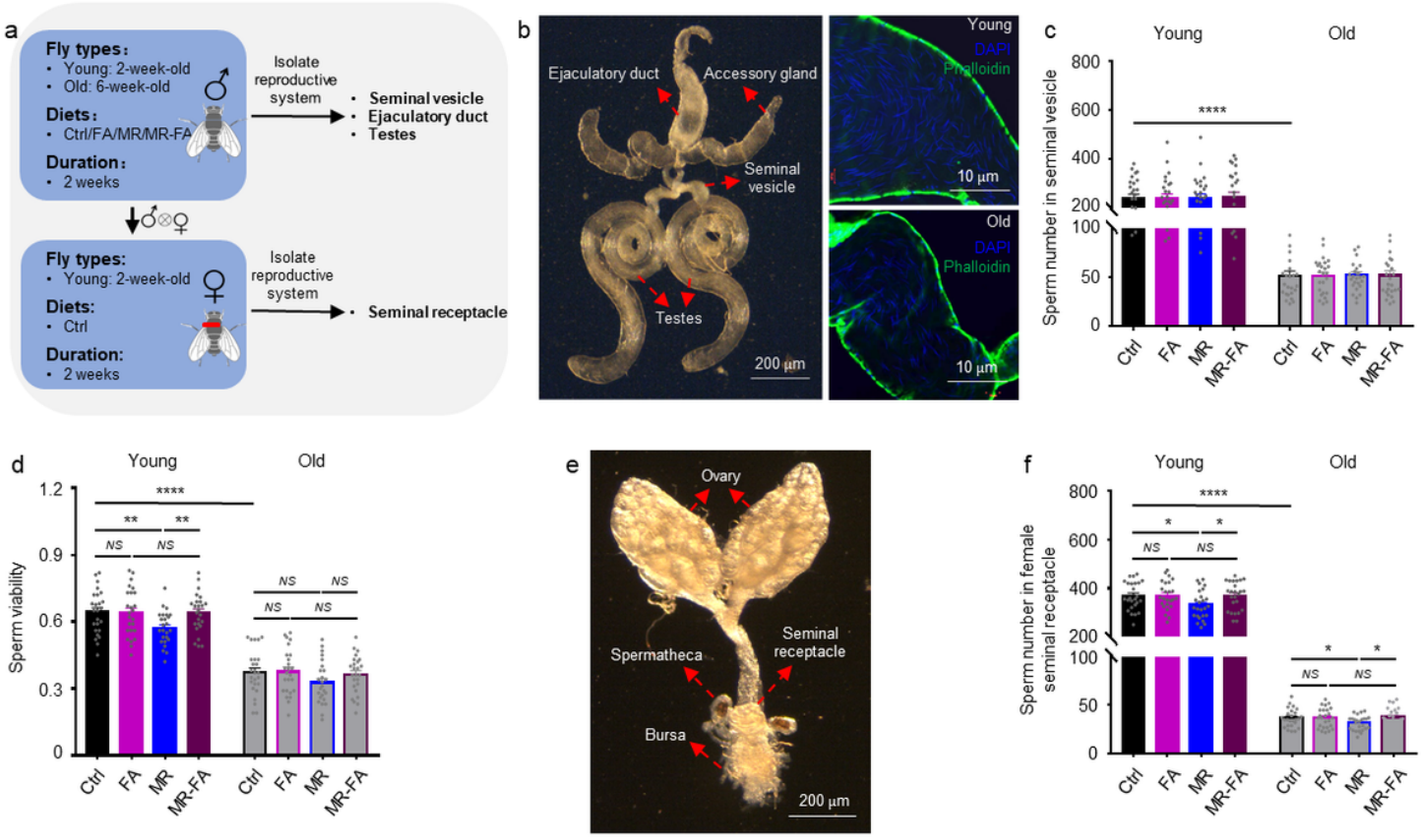

Figure 4

FA rescues MR-induced sperm viability and transfer decline. (a) Experimental design. (b) Reproductive system and seminal vesicle staining of male *Drosophila*. (c) Sperm number in seminal vesicle. (d) Sperm viability. (e) Reproductive system of female *Drosophila*. (f) Sperm number in seminal receptacle. n=25 flies per group. Scale bar, 200 μm (reproductive system) and 10 μm (seminal vesicle staining). Mean ± s.e.m. *NS* = *P*> 0.05, **P* < 0.05, ***P* < 0.01 and *****P* < 0.0001. *P* values were obtained by unpaired, two-tailed *t*-test.

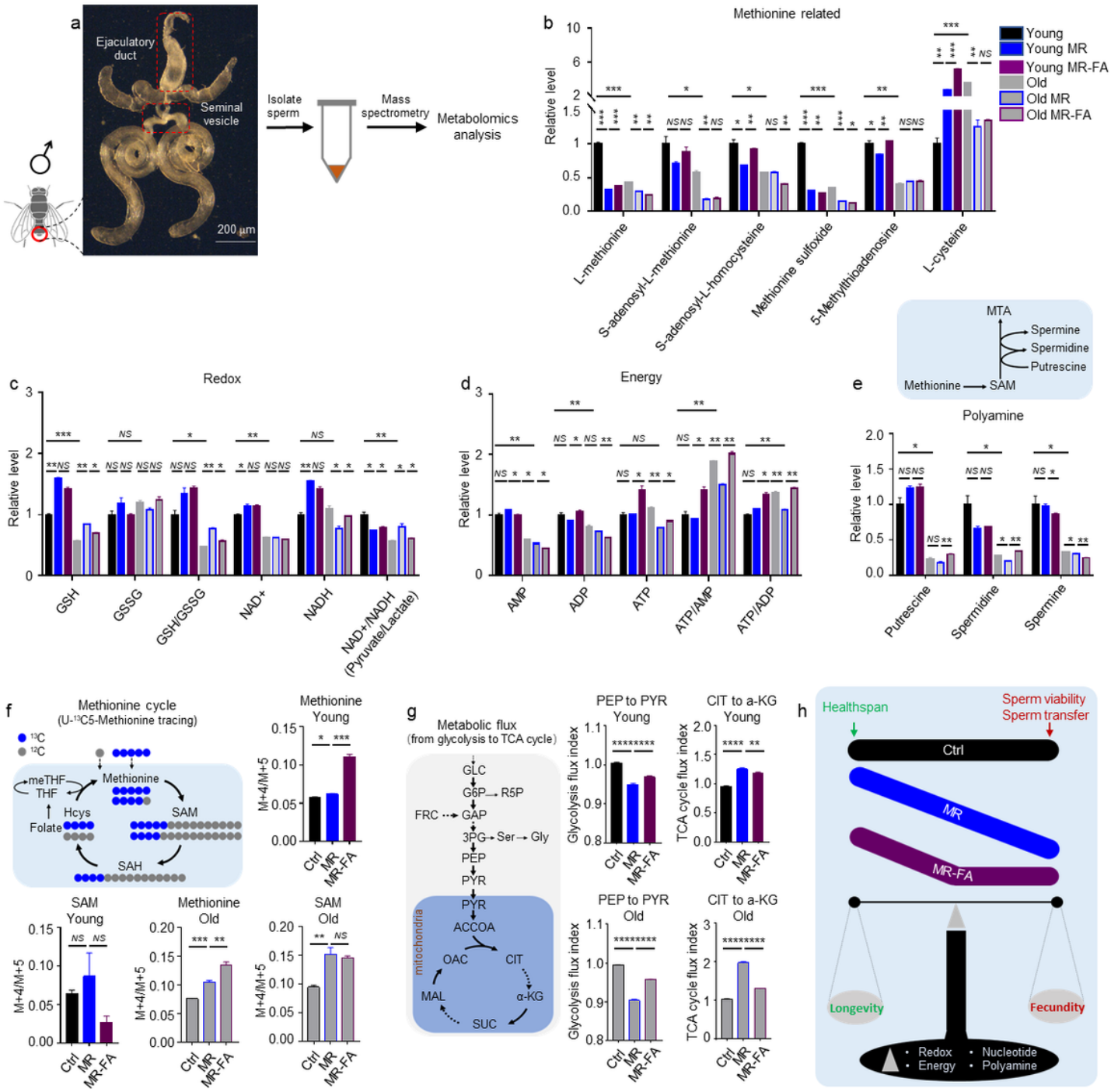

Figure 5

MR-FA maintains redox balance and enhances sperm energy metabolism. (a) Experimental design. (b-d) Metabolites related to methionine (b), redox balance (c) and energy state (d). (e) Metabolites related to polyamine metabolism. (f) Methionine cycle flux analysis. (g) Central carbon metabolic flux analysis. (h) Model. Green color represents lifespan and related factors; Brown color represents fertility and related factors; The triangle supporting the balance mainly contains redox balance, energy balance, nucleotide, and polyamine. Young flies n=30 and old flies n=90. Scale bar, 200 μm. Mean ± s.e.m. *NS* = $P > 0.05$, *$P < 0.05$, **$P < 0.01$, ***$P < 0.001$ and ****$P < 0.0001$. *P* values were obtained by unpaired, two-tailed *t*-test.

Supplementary Files

This is a list of supplementary files associated with this preprint. Click to download.

- ExtendedDataFiguresTables.docx